J Solid State Electrochem
DOI 10.1007/s10008-015-3018-1

ORIGINAL PAPER

Efficiency enhancement by mixed cation effect in polyethylene oxide (PEO)-based dye-sensitized solar cells

M. A. K. L. Dissanayake [1,2] · **E. M. B. S. Ekanayake** [2,3] · **L. R. A. K. Bandara** [2] · **V. A. Seneviratne** [2] · **C. A. Thotawatthage** [1] · **S. L. Jayaratne** [1] · **G. K. R. Senadeera** [1,4]

Received: 5 June 2015 / Revised: 30 July 2015 / Accepted: 13 August 2015

Abstract The enhancement in efficiency of N719 dye-sensitized solar cells (DSSCs) by a mixed cation iodide salt mixture is investigated. The gel electrolyte used in the glass/FTO/nano-porous TiO_2/gel electrolyte, I_2/Pt/FTO/glass solar cell structure, consists of tetrapropylammonium iodide (Pr_4NI) and potassium iodide (KI) in a plasticized polyethyleneoxide (PEO) host. The salt composition is varied to optimize the efficiency. With 100 wt% KI and 100 wt% Pr_4NI efficiencies under AM 1.5 illumination are 3.75 and 3.13 %, while 66.7 w% KI composition shows the highest efficiency of 4.44 %. This is an efficiency enhancement of about 18 %. DC polarization measurements established the predominantly ionic behavior of the electrolytes. Results also show that the variation of efficiency with salt composition essentially followed the same trend as the variation of short circuit photocurrent density (J_{SC}), which appears to be governed by the iodide ion conductivity. The above observations are further supported by photovoltage decay measurements where the electron recombination life time, τ_e, has the smallest value for the highest efficiency solar cell.

Keywords Dye-sensitized solar cells · Efficiency enhancement · Mixed cation effect · PEO-based gel electrolyte

Introduction

After the first report by O'Regan and Grätzel in 1991, dye-sensitized solar cells (DSSCs) have been extensively studied and developed due to their lower fabricating cost, simpler technology, and reasonably higher efficiencies [1–3]. A DSSC generally consists of a working electrode with a dye-adsorbed nanocrystalline titanium dioxide (TiO_2) layer, an electrolyte containing iodide/tri-iodide (I^-/I_3^-) redox couple, and a counter electrode comprising a catalytic platinum film.

DSSCs consisting of electrolyte solutions typically have efficiencies around 10 % but suffer from several major drawbacks, such as the lack of long-term stability due to liquid leakage, usage of volatile liquids such as acetonitrile, electrode corrosion, and photodecomposition of the dye in the solvent medium. In order to overcome these problems, many attempts have been made to replace the liquid electrolyte by quasi-solid or gel polymer electrolytes [4–7].

Solid polymer electrolytes are ionic conductors formed by dissolving ionic salts in suitable high molecular weight polymers such as poly(ethylene oxide) (PEO) and poly(propylene oxide) (PPO) [8]. However, due to their low ambient temperature conductivity, it has not been possible to use solid polymer electrolytes successfully in practical devices such as lithium rechargeable batteries and dye-sensitized solar cells. One of the commonly used strategies to increase the ambient temperature conductivity of polymer electrolytes is to incorporate plasticizers so that the resulting "gel" electrolyte will have

✉ M. A. K. L. Dissanayake
makldis@yahoo.com

[1] Institute of Fundamental Studies, Hantana Road, Kandy, Sri Lanka

[2] Department of Physics, University of Peradeniya, Peradeniya, Sri Lanka

[3] Postgraduate Institute of Science, University of Peradeniya, Peradeniya, Sri Lanka

[4] Department of Physics, The Open University of Sri Lanka, Nawala, Nugegoda, Sri Lanka

sufficiently high conductivity for practical applications. These polymer gel electrolytes can generally be made by using plasticizers in polyethyleneoxide (PEO)-based systems where the ether oxygen atoms facilitate the cation transport mechanism and the anion transport occurs by diffusion. Polymer gel electrolytes can also be made by using an organic solution electrolyte "entrapped" within a matrix formed by polymers such as polyacrylonitrile(PAN) and polymethylmethacrylate (PMMA) where the polymer host essentially acts as a matrix [9, 10].

Polyethyleneoxide (PEO) has the ability to solvate a variety of inorganic salts leading to polymer electrolytes with significant values of ionic conductivity. PEO and most PEO-salt mixtures exhibit co-existence between crystalline and amorphous phases; in fact, only 15–30 % of PEO is in the amorphous phase at room temperature. Most PEO-based polymer electrolytes that have been widely studied so far are solvent-free complexes of high molecular weight PEO and alkali metal salts, developed as cationic conductors, mainly as Li^+ conductors for rechargeable lithium batteries [8, 11]. Plasticizers such as ethylene carbonate (EC) and propylene carbonate (PC) are able to reduce the crystallinity of the PEO polymer and lower the glass transition temperature T_g in order to enhance the ambient temperature ionic conductivity of PEO-salt complexes [12–14]. There are not many reports of PEO-based anionic conductors. Due to the high polarity to dissolve redox couples such as I^-/I_3^- and excellent chemical stability, these can be developed as iodide (I^-)- and tri-iodide (I_3^-)-conducting electrolytes to be used in dye-sensitized solar cells [15–20].

In DSSCs based on iodide ion-containing gel electrolytes, the contribution of the iodide and tri-iodide ion (I^-,I_3^-) conductivity to the overall ionic conductivity is a major factor which determines the short circuit photocurrent density (J_{sc}) and hence the efficiency. This is because the iodide and tri-iodide ions, while participating in the I^-/I_3^- redox reactions, also shuttle between the photo-electrode and the counter electrode. During the solar cell action, the iodide ions (I^-) migrates from the Pt counter electrode to the dye-sensitized TiO_2 photoanode while the tri-iodide ions (I_3^-) migrate from the TiO_2 electrode to the Pt counter electrode. Although iodide ion conductivity plays an important role in determining the short circuit photocurrent and the efficiency of a DSSC, not much systematic research work has been reported on this subject.

Several studies have revealed that cations in the electrolyte, when adsorbed to the TiO_2 semiconductor surface, have a profound influence not only in determining the short circuit current density (J_{sc}) but also on the electron dynamics at the electrolyte/semiconductor interface and hence on the efficiency of DSSCs [21–24]. Central to many cation effects is the influence of the interfacial cation concentration on semiconductor energetics. In liquid electrolytes and in some polymer electrolytes, different cations have shown different effects on open circuit voltage, V_{oc} [24].

Although electrolytes with many different types of single cation salts have been used in DSSCs, there are only very few published reports on the use of a mixed cation binary iodide salt mixture as the iodide source. Electrolytes with a single iodide salt containing small size cations such as LiI, KI, MgI_2 as well as quaternary ammonium salts containing bulky cations such as tetrapropylammonium iodide (Pr_4NI) and tetrahexylammonium iodide (Hex_4NI) have been widely used in the past to provide iodide ions in DSSCs. While small-sized cations, such as Li^+ and K^+, are expected to enhance the short circuit photocurrent at the expense of the open circuit voltage, bulky cations such as Pr_4N^+ and Hex_4N^+ have shown to minimize the drop in photovoltage caused by cation adsorption on TiO_2 electrode [25, 26].

There are few reports on DSSCs with iodide salt mixtures showing better performance compared to those with only one iodide salt [27, 28]. In some reports, DSSCs containing aqueous electrolytes with various cations have shown that short circuit current density increases with the increasing charge density of the cation in the electrolyte while the fill factor, open circuit voltage, and efficiency decrease [29, 30]. Because of the seemingly different roles played by different size cations in affecting the J_{sc} and V_{oc} and electron dynamics at the semiconductor/electrolyte interface, it would be interesting to explore the combined effect of using a binary mixture of two iodide salts, one consisting of a bulky cation and the other consisting of a small alkali cation with different charge densities in the electrolyte in order to benefit from both cation types/sizes. Accordingly, we have studied the present DSSC system using the Pr_4NI and KI as the mixed cation binary iodide mixture incorporated into the PEO-based gel polymer. The beneficial effect of using this type of binary iodide salt mixture with mixed cations on the efficiency enhancement in several quasi-solid state DSSCs with PAN-based and PMMA-based gel electrolytes have already been reported by us [31–33]. As far as we are aware, this is the first report of a DSSC employing a PEO-based polymer gel electrolyte containing a small cation (K^+) and a bulky quaternary ammonium cation (Pr_4N^+), emphasizing cation size effect and the iodide ion conductivity on solar cell performance.

Experimental

Materials

All the chemicals used as starting materials were of purity greater than 98 %. Polyethylene oxide (PEO, Mw 4×10^6, Aldrich), ethylene carbonate (EC) (Fluka), propylene carbonate (PC) (Fluka), tetrapropylammonium iodide (Pr_4NI) (98 %, Aldrich), potassium iodide (KI) (99.5 %, Fluka), iodine (Fluka), glacial acetic acid (99 %, Fisher scientific), Triton-X (Aldrich), and ethanol (BDH) were used as received. Titanium dioxide powder (TiO_2) (P-25) was purchased from Degussa AG. Fluorine-doped tin oxide glass plates (FTO) (Nippon glass of sheet resistance 10–12 Ω/sq) were used as a substrate for coating TiO_2 paste. Ruthenium dye (N719)(ditetrabutylammoniumcisbis(isothiocyanato)bis(2,2′-bipyridyl-4,4′ dicarboxylicacid) purchased from Solatronix was used as the sensitizer. All the chemicals except I_2 and PC were vacuum dried at 60 °C for 24 h prior to use.

Preparation of the PEO-based gel electrolyte

For the preparation of the electrolyte samples, the weight of PEO (0.10 g), EC (0.40 g), and PC (0.40 g) was kept unchanged while the total weight of KI and $Pr_4N^+I^-$ was kept at 0.06 g. The weight of the I_2 was taken to be one tenth of the mole amount of the iodide salt. Weighed amount of EC, PC, Pr4NI, and KI was magnetically stirred at room temperature in a closed bottle for 30 min for complete dissolution of all the salts. Appropriate amount of PEO was then added, and the mixture was magnetically stirred at 140 °C on a hot plate for 1 h until the entire polymer has been dissolved. Subsequently, the mixture was allowed to cool down to room temperature and appropriate amount of iodine was added. The mixture was then continuously stirred for overnight to obtain the gel polymer electrolyte. The above procedure was repeated for all six compositions shown in Table 1.

Conductivity measurements

Ionic conductivity of the gel polymer electrolyte samples was determined by the AC complex impedance method using a Solatron SI–1260 impedance analyzer in the frequency range 20 Hz–10 MHz. Sample was placed inside a Teflon spacer and sandwiched between two polished stainless steel electrodes. The temperature of the sample was varied from about 25 to about 55 °C at approximately 5 °C intervals. The temperature of the sample was allowed to stabilize at each measuring temperature for about 30 min. For all the compositions studied, the ionic conductivity at each temperature was extracted from the corresponding impedance plots.

DC polarization measurements

The DC polarization test was performed for all six compositions by sandwiching each electrolyte sample between two stainless steel (SS) blocking electrodes and applying a small DC voltage of about 1 V and measuring the variation of the resulting current with time. This test was repeated for all the samples by sandwiching each sample between two iodine non-blocking iodine electrode pellets in the FTO/Pt/I_2/electrolyte/I_2/Pt/FTO configuration in order to estimate the iodide ion contribution to the total ionic conductivity.

TiO_2 electrode preparation

The TiO_2 paste was prepared by grinding 0.20 g of TiO_2 (Degussa P-25) with 12 drops (about 0.15 g) of glacial acetic acid, one drop (about 0.02 g) of triton X-100, and about 2 ml of ethanol. The resulting paste was spread on a pre-cleaned, fluorine-doped conducting tin oxide (FTO) glass (Nippon sheet glass, 10–12Ω/sq). An active cell area of 0.25 cm^2 was obtained by spreading the paste using the doctor blade technique and sintering at 450 °C for 45 min. The resulting TiO_2 nano-porous film was allowed to cool down to room temperature. The thickness of the film on FTO glass was measured with the help of a homemade, calibrated profilometer and the average film thickness of the TiO_2 film was found to be around 12 μm. Dye absorption was carried out by immersing the TiO_2 film in an ethanolic dye solution containing ruthenium dye N719 for 24 h.

Solar cell fabrication and characterization

The gel polymer electrolyte-based dye-sensitized solar cells (DSSCs) of configuration glass/FTO/TiO_2/dye/electrolyte,

Table 1 Compositions and parameters of solar cells with PEO:EC:PC: Pr_4NI+x wt% KI, I_2 gel electrolyte samples for six different KI/ Pr_4NI molar ratios

Weights: PEO:EC:PC: (KI+Pr_4NI) : I_2=0.1 g : 0.4 g : 0.4 g : (0.06 g) : x

x=0.1 of the molar weight of the iodide salts

Sample	A	B	C	D	E	F
KI wt%	0	16.6	33.3	50	*66.7*	100
V_{oc} (mV)	717.5	727.8	746.3	735.2	*742.4*	654.9
J_{sc} (mA cm^{-2})	7.68	9.26	9.48	9.68	*10.12*	9.36
Fill factor (%)	56.9	53.2	54.6	58.1	*59.1*	61.3
Efficiency (%)	3.13	3.58	3.86	4.14	*4.44*	3.75
Lifetime τ_e (s)	0.618	0.617	0.685	0.612	*0.529*	0.587

Italicize values refer to the electrolyte composition which gives the maximum solar cell efficiency

I_2/Pt/FTO/glass were fabricated by sandwiching the polymer electrolyte between the dye-adsorbed TiO_2 electrode and a platinum (Pt)-coated FTO glass. The photocurrent–voltage (*I*–*V*) characteristics of the cells were measured under the illumination of 100 mW cm^{-2} (AM 1.5) simulated sunlight using a computer-controlled measuring system coupled to a Keithley 2000 multimeter and a potentiostat/galvonostat HA-301. A Xenon 500 lamp was used with AM 1.5 filter to obtain the simulated sunlight with above intensity.

Photovoltage decay measurements

The solar cell was first set to open circuit state by setting the current in the Metrohm Autolab Potentiostat to zero. Then, the cell was illuminated by low intensity white light. After the cell reached the steady state, it was exposed to green laser light with wavelength 532 nm from a green LED. Then, the laser light was cut off by using a mechanical shutter. The resulting decay of the photo voltage with time was measured.

Results and discussion

Characterization of the PEO-based gel polymer electrolyte

The variation of ln σT vs 1/T for different electrolyte compositions is shown in Fig. 1. The electrolyte containing only Pr_4NI as the salt (sample A) has the lowest conductivity at all measured temperatures. It has a conductivity of 3.46×10^{-3} S cm^{-1} at 28 °C. At a given temperature, the conductivity gradually increases with the increasing amount of KI in the mixed salt electrolyte and the electrolyte containing 100 % KI (sample F) shows the highest conductivity of 6.94×10^{-3} S cm^{-1} at 28 °C. As seen in the Fig. 1, from the linear shapes, the conductivity appears to follow the Arrhenius equation,

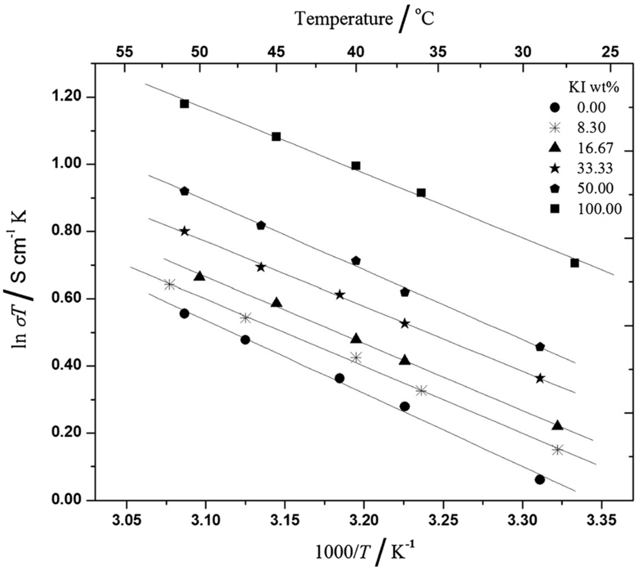

Fig. 1 The variation of lnσT plotted against the reciprocal absolute temperature for PEO/EC/PC/KI/Pr_4NI/I_2 gel electrolytes containing different KI/Pr_4NI weight ratios

$$\sigma T = B\exp\left(\frac{-E_\mathrm{a}}{kT}\right)$$

where E_a is the activation energy, *B* is the pre-exponential factor, and *k* is the Boltzmann constant.

A typical PEO-based polymer electrolyte has, in general, a multi-phase nature consisting of a pure PEO spherulite crystalline phase and an amorphous phase with dissolved salt. It has been accepted that significant ionic conduction in PEO-based polymer electrolytes occurs only in the amorphous elastomeric phase. Therefore, a key to the design of highly conducting PEO polymer electrolytes is to maximize the content of the amorphous phase [32–34]. During ion transport in a PEO polymer electrolyte, cations are coordinated with the oxygen atoms of the polyether chain. The ion transport mechanism consists of the cation migration facilitated by large amplitude segmental motion of the polymer chains. The anion is either indirectly weakly bound to the polymer chain through the bonding to cation or totally free and the anionic migration occurs by diffusion. However, the flexibility of the polymer chain is rate determining also for the anion transport. In a PEO-based polymeric electrolyte, the glass transition temperature, T_g, is lowered when plasticizers are incorporated indicating that the segmental mobility of PEO chains also increases resulting a faster ionic conduction. The plasticizers EC and PC added to PEO electrolytes will not only increase the amorphous nature of the PEO electrolyte but also promote the ionic dissociation into cations and anions. Both these would increase the ionic conductivity [34, 35]. While the high dielectric constant of the plasticizers favors salt dissociation, the low viscosity would lead to high ionic mobility.

Pulsed field gradient (PFG) NMR measurements of the cation and anion diffusion coefficients in the amorphous phase of the poly(ethylene) oxide-lithium triflate [$(PEO)_8LiCF_3SO_3$] complex have shown that there is a predominant anionic conductivity with a relatively high anionic transference number [36]. There are also reports indicating that the addition of EC and PC to PEO-based electrolytes would lead to an increase in anionic conductivity compared to the unplasticized electrolyte [37]. The Arrhenius-like behavior seen in Fig. 1 suggests that the mobility of ions is coupled more to the mobility of the organic solvents (EC/PC) and less to the segmental motion of the polymer chains. The activation energy values, which correspond to the gradients of the linear Arrhenius plots, are almost constant for all six gel electrolyte samples studied and essentially independent of the salt concentration ratios [KI]/[Pr_4NI].

The ionic conductivity of the sample F (with 100 wt% KI salt) originates from two types of ions, namely K^+ ions and I^-/I_3^-

ions, and all these ions contribute to the highest conductivity seen for this sample. On the other hand, the ionic conductivity of the sample with 100 wt% Pr_4NI (sample A) is the lowest. This must be expected as the cation Pr_4N^+ in this electrolyte sample is bulky in comparison to K^+ ion, and the iodide ions (I^-) are expected to make the dominant contribution to the ionic conductivity in this material. As the weight percentage of KI in the electrolyte increases from samples A to F, the dissociated K^+ and I^- ions from KI are expected to make a dominant contribution to the total ionic conductivity of the gel electrolyte because of the increased number of K^+ and I^- ions and high mobility of K^+ ions in comparison with the bulky Pr_4N^+ ions.

DC polarization data taken using stainless steel (SS) blocking electrodes show that all the gel electrolyte samples studied in this work are predominantly ionic conductors and the electronic conductivity is negligibly small. The steady-state DC polarization curves, taken with iodine pellet non-blocking electrodes in the SS/I_2/electrolyte/I_2/SS configuration for the gel electrolyte samples, PEO:EC:PC: Pr_4NI+x wt% KI, I_2 for different x values clearly show the different iodide ion (I^-) contributions to the overall ionic conductivity in each sample (curves not shown). From these measurements, it can be concluded that the iodide ion transference numbers for the six electrolyte samples are in the 0.15 to 0.45 range and follows the same trend as the variation of J_{sc}. This suggests that the anionic conductivity by I^- ions in the electrolyte, essentially determines the short circuit photocurrent density of the solar cell.

Characterization of dye-sensitized solar cell

The photocurrent–photovoltage (*I–V*) characteristics of six DSSCs of configuration glass/FTO/TiO_2/dye/electrolyte/Pt/FTO/glass were measured using gel electrolyte samples with seven different KI/ $Pr_4N^+I^-$ salt ratios (samples A to F). Although we have obtained *I–V* curves for solar cells with all six electrolyte compositions, only the curves for solar cells with three compositions are shown in Fig. 2 as representative examples. These three cells were fabricated with the gel electrolyte with 0 wt% KI (sample A), 66.7 wt% KI (sample E), and 100 wt% of KI (sample F). Solar cell parameters such as the open circuit voltage (V_{oc}) and the short circuit current density (J_{sc}) were measured and the fill factor (FF %) and efficiency (η %) were calculated for all the cells studied. The results are tabulated in Table 1.

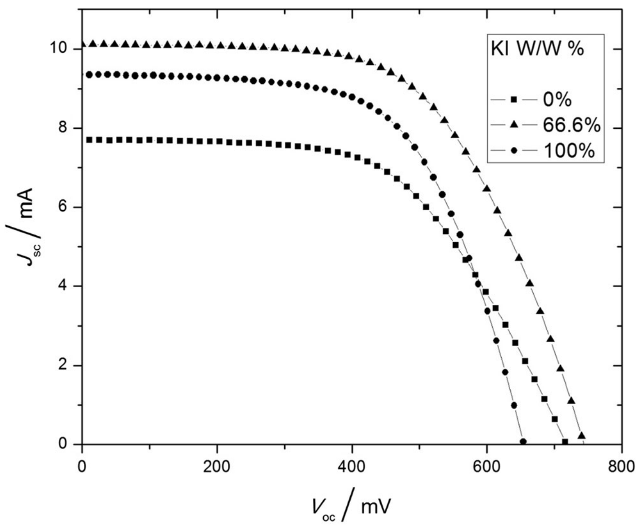

Fig. 2 The photocurrent–photovoltage (*I–V*) characteristics of three solar cells where the gel electrolyte salt compositions are 0 wt% KI (only Pr_4NI) (*black square*), 66.7 wt% KI+83.33 wt% Pr_4NI (*black triangle*), and 100 % KI (*black circle*). (100 mW cm^{-2}, A.M. 1.5, active area 0.25 cm^{-2})

The efficiency (η) and the short circuit current density (J_{sc}) of all six solar cells as a function of wt% KI are shown in Fig. 3. It is interesting to see that the efficiency variation follows a similar variation as the J_{sc}. It is important to realize that the solar cell fabricated with the binary iodide mixture with 66.7 wt% KI composition shows the highest energy conversion efficiency of 4.44 % and has the highest short circuit photo current density of 10.12 mA cm^{-2}, while the solar cells fabricated with 100 wt% KI and with 100 wt% Pr_4NI have shown efficiencies of 3.75 and 3.13 %, respectively. The use of the binary iodide mixture has clearly enhanced the solar cell efficiency by a factor of about 18 % compared to the cells with only a single iodide salt.

The power conversion efficiency (η %) of a solar cell is given by the following equation:

$$\eta = \frac{J_{\mathrm{SC}}\, V_{\mathrm{OC}}\, \mathrm{FF}}{\text{Total incident power density}}$$

where the symbols have their usual meanings. According to this formula and Table 1, the dominant contribution to the solar cell efficiency in the present work clearly comes from

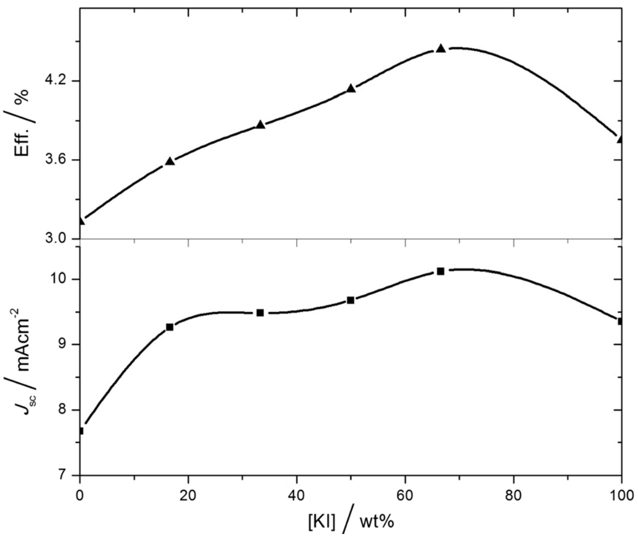

Fig. 3 The variation of **a** the efficiency (η) and **b** the short circuit photo current density (J_{sc}) of all six solar cells as a function of the wt% KI

the J_{sc} and is determined essentially by the relative amount of iodide ion conductivity in the PEO-based gel electrolyte.

Cation influenced charge transfer dynamics in DSSCs

Cations play an important role in the performance of DSSCs. The cation/TiO_2 interactions cause two effects in a DSSC; (i) a positive shift of the flat band potential of the semiconductor and (ii) the creation of deeper electron-trapping states, which play an important role in electron transport through TiO_2 to the current collector. The charge transfer process in a TiO_2-based dye-sensitized solar cell with a typical electrolyte containing an iodide/tri-iodide (I^-/I_3^-) redox couple involves several steps. Under light illumination, the photoexcited electrons are injected from the excited dye sensitizer (D*), ($D^* \rightarrow D^+ + e^-$) into the conduction band of the nanocrystalline TiO_2 and reach the external circuit. The oxidation of I^- anions ($3I^- \rightarrow I_3^- + 2e^-$) takes place on the surface of the dyed TiO_2 film, and therefore, the resulting dye cations in the previous step are reduced by I^- anions ($2D^+ + 3I^- \rightarrow 2D + I_3^-$). Meanwhile, the oxidized I_3^- species migrate from the photoanode to the platinized counter electrode and become reduced to I^- by accepting electrons from the external circuit. Cations in the electrolyte can efficiently screen the photo-injected electrons on the TiO_2 film, ensuring that electro-neutrality is maintained throughout the TiO_2 network. Ionic migration in an electrolyte is therefore strongly correlated with electron transport in the TiO_2 film. The dependence of J_{sc} and V_{oc} on the type, size, and the nature of the cation take place due to interfacial kinetics of the dyed TiO_2 film. Upon light illumination of the dyed nanoporous TiO_2 film, the injected electrons from the excited dye molecules are accumulated at the conduction band of TiO_2, and the cations in the electrolyte become adsorbed into the TiO_2 film for charge compensation. The V_{oc} is determined by the relative positions of the flat band potential and the redox potential of the electrolyte ($V_{oc} = |V_{fb} - V_{red}|$). The flat band potential of TiO_2 is moved positively due to the cation adsorption, and it is associated in the drop in photovoltage of the DSSC. The associated drop in photovoltage depends upon the size and charge density of the cations. As compared to the bulky cations, small-sized cations could easily be adsorbed on to the TiO_2 grain surface producing a larger potential drop. However, due to this greater positive shift of the TiO_2 flat band potential, the driving force for the charge injection from the excited dye molecules to TiO_2 increases, resulting greater injection efficiency and thus a higher photocurrent.

The mixed cation effect

We find that only very few studies are reported in the literature on the use of mixed cation iodide salt mixtures emphasizing on the effect of cations on the performance of DSSCs. For the binary iodide system LI+KI in a PEO-based gel electrolyte, the maximum solar cell efficiency of 4.5 % has been achieved at 14.5 wt% of KI [27]. In this system, the short-circuit photocurrent density (J_{sc}) has reached a maximum at 14.5 wt% KI concentration. However, these authors have not attempted to correlate the solar cell efficiency directly with the J_{sc} and the iodide ion conductivity in the electrolyte.

The influence of single iodide salts with different size cations on the performance of dye-sensitized solar cells has been studied by several groups. The general finding is that small radius cations such as Li^+ and K^+ get intercalated into the lattice of nano TiO_2 causing a positive shift of the conduction band edge potential. This increases the driving force for charge injection and typically leads to a higher J_{sc} at the expense of V_{oc}. This effect is much lower with iodide salts having bulky cations such as Pr_4N^+ [30, 38, 39]. It is interesting to note that the J_{sc} and V_{oc} values of the two end members in our binary iodide system are generally consistent with the reported data for single cation salts. In the present system, the J_{sc} value is 7.68 mA cm^{-2} for the 100 wt% Pr_4NI system which is lower than the J_{sc} value of 9.36 mA cm^{-2} for the 100 wt% KI system (Table 1). In the present system, the adsorption of cations, K^+ and Pr_4N^+ ions, on the surface of nano titania grains would cause the conduction band edge to move to the positive side (downward shift) independent of the cation charge density, thereby decreasing the V_{oc} values. This effect is expected to be more pronounced for smaller K^+ ions (ionic radius, 0.138 nm) than for bulky Pr_4N^+ ions (ionic radius, 0.46 nm) as the number of adsorbed K^+ cations per unit area of nano titania grain surface would be much greater than the number of Pr_4N^+ ions adsorbed due to the difference in their sizes. Therefore, the drop in V_{oc} due to this effect should be greater for the solar cell with electrolyte with 100 wt% KI concentration (sample F) compared to the drop in V_{oc} for the cell with 100 wt% Pr_4NI electrolyte (sample A). This can be clearly seen from the V_{oc} values given in Table 1.

The occurrence of the maxima in the efficiency and J_{sc} at 66.7 wt% KI concentration can be explained as follows. The net iodide ion concentration [I^-] in the gel electrolyte results from the dissociation of both ionic salts. From our calculations, it could be seen that the net iodide ion concentration resulting from ionic dissociation of both salts increases from the 0 wt% KI end to the 66.7 wt% KI sample, giving rise to an initial increase in J_{sc} (Fig. 3). At these low iodide ion concentrations, one can expect that all the available iodide ions (I^-) to be free and to contribute to the J_{sc} and efficiency. The maximum efficiency and the maximum J_{sc} occur at the optimized relative molar iodide ion concentration which corresponds to sample E with 66.7 wt% KI. According to DC polarization data (not shown), this composition also had the highest iodide ion transference number of 0.45. Beyond the 66.7 wt% KI composition, the efficiency as well as the J_{sc} drops despite the increase in iodide ion concentration in the electrolyte. Clearly, a major factor which contributes to this decrease in iodide ion conductivity is the decrease in the number of free iodide ions due to the formation of ion–ion pairs and higher ionic aggregates. A similar trend has been observed by other researchers in studies on lithium salt in PEO-based polymer electrolyte systems using the concept of ion association and the formation of charge multiplets as well as due to the decrease in ionic mobility due to increased viscosity in the medium [40].

A NMR study on ionic conductivity and self-diffusion coefficient of lithium ions and the behavior of ion association in the plasticized PEO: $LiClO_4$ system has shown that, above a certain salt concentration, the fraction of "free" anions decreases with increasing salt concentration [41]. However, in PEO:PC gel electrolytes containing lithium salts, it has been reported that the diffusion of lithium ions increases as the salt concentration increases in the gel [42].

The results from literature as discussed above agree well with our observations made on the present system (Fig. 1). While at higher KI salt concentrations beyond the J_{sc} maximum, the total ionic conductivity keeps on increasing with increased KI wt% evidently due to the contribution by highly mobile K^+ ions, the iodide ion (I^-) conductivity contribution and hence the J_{sc} decreases after exhibiting the maximum at 66.7 wt% KI. Evidently, at these high I^- ion concentrations, a considerable fraction of iodide ions remain in the electrolyte as neutral aggregates without participating in ionic transport, although, the overall ionic conductivity continues to increase gradually (see Fig. 1) largely due to the increase in the number of K^+ ions.

Several factors need to be considered in order to explain the observed trends in J_{sc} and V_{oc} in these solar cells with mixed cation-based electrolytes. The J_{sc} is determined not only by the enhanced driving force due to increased potential difference (downhill for electrons) caused by small cations adsorbed by the TiO_2 layer but also by the iodide ion conductivity in the electrolyte medium. As we can clearly see from Fig. 3, the shift of conduction band edge caused by the adsorption of K^+ ions and the resulting enhanced electron transfer from the dye to the TiO_2 conduction band appears to be the dominant mechanism up to the 66.7 % KI concentration which determines the J_{sc} and hence the efficiency. All the photogenerated electrons can contribute to the redox reaction at the TiO_2/electrolyte interface, and due to the high iodide ion conductivity (and iodide ion transference number) up to this KI composition, the J_{sc} will reach its maximum value. This is the "rate-determining" mechanism up to 66.7 % KI concentration. However, as the KI concentration increases beyond this optimum value, the rate-determining mechanism will be the iodide ion conductivity (and iodide ion transference number) and not the rate of generation of photoelectrons. Therefore, the J_{sc} value and hence the efficiency will be decreasing beyond 66.7 wt% KI concentration, up to 100 wt% KI concentration. The reason for the decrease in J_{sc} is the decrease in iodide ion conductivity due to the formation of ion pairs and higher ionic aggregates and also increased viscosity due to high KI concentration at the expense of dissociated free iodide ions. In these high KI concentrations, although the total amount of iodine in the medium is high, the number of I^- ions actually contributing to the solar cell performance through J_{sc} is less compared to the optimized KI concentration. At these high KI concentrations, the high total conductivity is due to the K^+ ions, as evidenced from the low iodide ion transference number.

In summary, the J_{sc} (and hence the efficiency) will be determined by the competition between the effect of energy band shift by cation adsorption and the iodide ion concentration in the electrolyte. The former will be rate determining at low KI concentrations and the latter at high KI concentrations.

In order to confirm our observations, we have performed photovoltage decay measurements under open circuit conditions independently on all the six DSSCs and only the variation of V_{oc} as a function of time for three DSSCs are shown in Fig. 4. Under these conditions, the photogenerated electrons will combine with I_3^- in the redox electrolyte after a time τ_e as described below. The three DSSCs shown include the two end members and the highest efficiency member. The curves through the data points are fits to a single exponential decay process according to $\exp(-t/\tau_e)$, where τ_e is the apparent electron recombination life time. τ_e represents the length of time photogenerated electrons remain in the film before interacting with I_3^- ions at the TiO_2/electrolyte interface under open circuit conditions. The extracted τ_e values from curve fitting are given in Table 1. The fastest voltage decay with smallest τ_e corresponds to the highest efficiency cell with highest J_{sc} (maximum). From Table 1 and Fig. 4, it is clear that τ_e

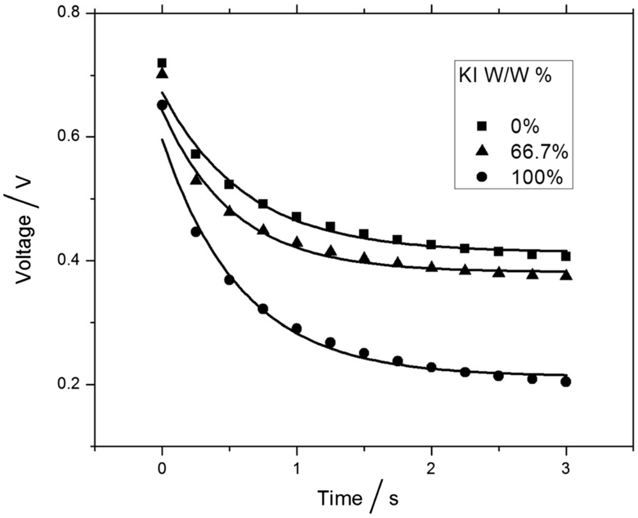

Fig. 4 The variation of voltage decay as a function of time for three solar cells with electrolyte compositions 0 wt% KI (only Pr_4NI) (*black square*), 66.7 wt% KI+83.33 wt% Pr_4NI (*black triangle*), and 100 % KI (*black circle*)

decreases with increase in tri-iodide ion (I_3^-) concentration. Sufficient I_3^- ions are available to reduce the dye cations, and therefore, the decrease in τ_e is directly related to increase of I^-/I_3^- concentration. The lifetime of an electron in the TiO_2 electrode should decrease with the increasing of the concentration of I_3^- in the electrolyte, because the probability of encountering electrons in the TiO_2 electrode with I_3^- increases with the increasing of I_3^- concentration. This is consistent with the results from the present work where the lowest electron lifetime corresponds to the highest iodide ion concentration at 66.7 wt% KI. This interpretation is analogous to the analysis given in reference [43] for a PVDF-HFP-based solar cell.

Conclusions

In dye-sensitized solar cells, fabricated with PEO-based gel polymer electrolyte incorporating a mixed cation iodide system consisting of a small alkali cation (K^+) and a bulky cation (Pr_4N^+), the variation of efficiency with wt% KI follows a similar variation as the J_{sc} which appears to be governed by the iodide ion conductivity in the electrolyte. The dependence of the short circuit photocurrent and the open circuit photovoltage on the cation type of the two end member compositions generally agrees with reported data for related single cation systems. The maximum efficiency and the maximum in J_{sc} occurs at 66.7 wt% KI concentration. With identical electrolyte compositions, the solar cell with 100 wt% KI showed an efficiency of 3.75 % and the cell with 100 wt% Pr_4NI showed an efficiency of 3.13 %. However, the cell with the mixed iodide system with 66.7 wt% KI concentration showed the highest efficiency of 4.44 % which corresponds to the maximum in J_{sc} of 10.75 mA cm^{-2}. The above observations are further supported by photovoltage decay measurements where the electron recombination life time, τ_e, has the smallest value for the highest efficiency solar cell with highest concentration of iodide (I_3^-) ions. We believe that the efficiency enhancement by about 18 % and the occurrence of the maxima in the solar cell efficiency and the short circuit photocurrent at an optimum iodide ion concentration is an important finding.

The observed efficiency enhancement achieved by employing the mixed cation iodide mixture in the gel electrolyte instead of a single iodide salt could be utilized in different types of dye-sensitized solar cell systems using polymeric, gel, and even solution electrolytes to increase the efficiency by a considerable percentage, which we believe is quite significant in DSSC research.

Acknowledgments The authors wish to thank the International Programme in the Physical Sciences (IPPS), Uppsala University, Sweden, National Institute of Fundamental Studies, Kandy, Sri Lanka, University of Peradeniya, and the Postgraduate Institute of Science (PGIS), Sri Lanka for numerous research support and for making the facilities available to carry out this project.

References

1. O'Regan B, Grätzel M (1991) Nature 353:737–740
2. Hagfeldt A, Grätzel M (1995) Chem Rev 95:49–68
3. Grätzel M (2001) Nature 414:338–344
4. Dissanayake MAKL, Bandara LRAK, Bokalawela RSP, Jayathilaka PARD, Ileperuma OA, Somasundaram S (2001) Mat. Res Bull 37:867–874
5. Roh DK, Chi WS, Jeon H, Kim SJ, Kim JH (2014) Adv Functional Mater 24:379–386
6. Yang H, Huang M, Wu J, Lan Z, Hao S (2008) Mater Chem Phys 110:38–42
7. Bandara TMWJ, Dissanayake MAKL, Mellander B-E (2010) Electrochim. Acta 55(6)15: 2044-2047
8. MacCallum JR, Vincent CA (eds) (1987) Pol Elect Rev vol 1 Elsevier Applied Science, London
9. Stephan AM (2006) Eur Polym J 42:21–42
10. Jayathilaka PARD, Dissanayake MAKL, Albinsson I, Mellander B-E (2003) Solid State Ionics 156:179–195
11. Wright PV (1975) Br Polym J 7:319–327
12. Watanabe M, Kanba M, Matsuda H, Tsunemi K, Mizoguchi K, Tsuchida E, Shinohara I (1981) Makromol Chem Rapid Commun 2:741–744
13. Pitawala HMJC, Dissanayake MAKL, Seneviratne VA (2007) Solid State Ionics 78:885–888
14. Kang M-S, Kim JH, Won J, Kang YS (2006) J Photochem Photobiol A Chem 183:15–21
15. Kalaignan GP, Kang M-S, Kang YS (2006) Solid State Ionics 177: 1091–1097
16. Singh PK, Kim K-I, Park-G, Rhee H-W (2007) Macromolecular Symposia 162-166
17. Yang Y, Zhou C-H, Xu S, Hu H, Chen B-L, Zhang J, Wu S-J, Liu W, Zhao X-Z (2008) J Power Sources 185:1492–1498
18. Shen X, Xu W, Xu J, Liang G, Yang H, Yao M (2008) Solid State Ionics 179:2027–2030
19. Bandara TMWJ, Dissanayake MAKL, Ileperuma OA, Varaprathan K, Vignarooban K, Mellander B-E (2008) J Solid State Electrochem 12:913–917
20. Ilepruma OA, Dissanayake MAKL, Somasundaram S, Bandara LRAK (2004) Sol. Energy Mater Sol Cells 84:117–124
21. Watson DF, Meyer GJ (2004) Coord Chem Rev 248:1391–1406
22. Kelly CA, Farzad F, Thompson DW, Stipkala JM, Meyer GJ (1999) Langmuir 15:7047–7054
23. Kambe S, Nakade S, Kitamura T, Wada K, Yanagida S (2002) J Phys Chem B 106:2967–2972
24. Liu Y, Hagfeldt A, Xiao XR, Lindquist SE (1998) Sol Energy Mater Sol Cells 55:267–281
25. Chen J, Peng T, Fan K, Xia J (2011) J Mater Chem 21:164 48-16452
26. Li P, Wu J, Hao S, Lan Z, Li Q, Huang Y (2011) J Appl Polym Sci 120:1752–1757
27. Agarwala S, Thummalakunta LNSA, Cook CA, Peh CKN, Wong ASW, Ke L, Ho GW (2011) J Power Sources 196:1651–1656
28. Abraham KM, Alamgir M (1990) J Electrochem Soc 137:1657–1658
29. Graetzel M (2005) Inorg Chem 44:6841–6851
30. Shi Y, Wang Y, Zhang M, Dong X (2011) Phys Chem Chem Phys 13:14590–14597
31. Dissanayake MAKL, Thotawatthage CA, Senadeera GKR, Bandara TMWJ, Jayasundera WJMJSR, Mellander B-E (2012) J Photochem Photobiol A Chem 246:29–35
32. Bandara TMWJ, Dissanayake MAKL, Jayasundera WJMJSR, Albinsson I, Mellander B-E (2012) Phys Chem Chem Phys 14: 8620–8627
33. Armand MB (1986) Annu Rev Mater Sci 16:245–261

34. Gray FM (1991) Solid Polymer Electrolytes VCH New York 245
35. Berthier C, Gorecki W, Minier M, Armand MB, Chabagno JM, Rigand P (1983) Solid State Ionics 11:91–95
36. Bhattacharja S, Smoot SW, Whitmore DH (1986) Solid State Ionics 18–19:306–314
37. Kim Y-T, Smotkin ES (2002) Solid State Ionics 149:29–37
38. Lee S-H A, Jackson A-M S, Hess A, Fei S-H, Pursel SM, Basham J, Grimes CA, Horn MW, Allcock HR, Mallouk TE (2010) J Phys Chem C 114:15234–15442
39. Park N-G, Chang S-H, Van de Lagemaat J, Kim K-J, Frank AJ (2000) Bull Kor Chem Soc 21:985–988
40. Doeff MM, Edman L, Sloop SE, Kerr J, De Jonghe LC (2000) J Power Sources 89:227–231
41. Kao H-M, Chang P-C, Chao S-W, Lee C-H (2006) Electrochim Acta 52:1015–1027
42. Hayamizu K, Aihara Y, Arai S, Price WS, Electrochim Acta 45: 1313-1319
43. Lee K-M, Suryanarayanan V, Ho K-C (2008) J Power Sources 185: 1605–1612